

Accepted Manuscript

Title: Characterization and photocatalytic activity of N – doped TiO₂ prepared by thermal decomposition of Ti – melamine complex

Authors: M. Sathish, B. Viswanathan, R.P. Viswanath

PII: S0926-3373(07)00079-3
DOI: doi:10.1016/j.apcatb.2007.03.003
Reference: APCATB 9935

To appear in: *Applied Catalysis B: Environmental*

Received date: 23-1-2007
Revised date: 28-2-2007
Accepted date: 7-3-2007

Please cite this article as: M. Sathish, B. Viswanathan, R.P. Viswanath, Characterization and photocatalytic activity of N – doped TiO₂ prepared by thermal decomposition of Ti – melamine complex, *Applied Catalysis B, Environmental* (2007), doi:10.1016/j.apcatb.2007.03.003

This is a PDF file of an unedited manuscript that has been accepted for publication. As a service to our customers we are providing this early version of the manuscript. The manuscript will undergo copyediting, typesetting, and review of the resulting proof before it is published in its final form. Please note that during the production process errors may be discovered which could affect the content, and all legal disclaimers that apply to the journal pertain.



**CHARACTERIZATION AND PHOTOCATALYTIC ACTIVITY OF N – DOPED
TiO₂ PREPARED BY THERMAL DECOMPOSITION OF Ti – MELAMINE
COMPLEX**

M. Sathish, B.Viswanathan and R.P.Viswanath*

Department of Chemistry, Indian Institute of Technology Madras, Chennai-600 036.India

E.mail: rpv@iitm.ac.in

Phone: 91- 44-64540460; Fax: 91-44-22574200

Abstract

Nitrogen doped spherical TiO₂ has been prepared by thermal decomposition of Ti-Melamine complex in air atmosphere. A clear shift in the onset light absorption from UV region (<400) to visible region (>520 nm) has been observed for the N-doped samples. It has been deduced from the optical absorption spectra that the higher calcination temperature results in the decreases of amount of N-doping. The XRD results revealed the phase transition of TiO₂ from anatase to rutile crystalline phase, starting at calcination temperature ≥ 600 °C. The electron microscopic images reveal the formation of spherical and flakes of TiO₂ nanocrystals (25 nm). The chemical nature of N in the N-TiO₂ has been evolved through X-ray photoelectron spectroscopy. The presence of different types of N species have been observed corresponding to different oxidation state and the presence of Ti-N and O-Ti-N environment has been confirmed from the observed binding energy values. Photocatalytic decomposition of methylene blue has been carried out both in the visible region and UV+Visible region. N-TiO₂ showed higher activity compared to the undoped commercial TiO₂ (Degussa P25) photocatalyst in the visible region.

Keywords: N-doped TiO₂, anion doping, photocatalysis, visible light absorption

Introduction

Titanium dioxide, the promising photocatalyst receives incessant attention so far from their earliest invention by the Japanese scientists in 1972 [1]. Though, it is active only in the UV region, the other properties like stability against photocorrosion, moderate band gap and suitable band position, easy availability, safe and low cost, etc makes this material as foremost one among the available photocatalysts. Recently, various attempts have been made to improve the visible light activity. Various noble/transition metal (or) metal ions have been doped into the TiO₂ lattice and the photocatalytic activity has been studied [2, 3], but none of them has given satisfactory results. In particular, the stability, low inter particle electron transfer rate, photocorrosion of the dopant, and harmful nature of the doped materials are some of the drawbacks. It is conceived from the literature knowledge that the modification of the band structure is essential to alter the light absorption characteristics of the TiO₂. With this in view, the research has been focused to modify its band structure in such a way that the electron-hole pair are created on the valence band (VB) and conduction band (CB) of the TiO₂ by absorbing the light from visible region. At the same time, it should be kept in mind that, the band edge position that is in the top of the valence band and bottom of the conduction position should not be altered exceedingly. This may diminish the reduction and oxidation capability of the TiO₂ photocatalyst. Among the various methods tried, the recent preliminary studies on doping of non-metals like N, S, C on TiO₂ lattice has opened a new door in the non-metal doping with significant expectation [4-20]. Also, it is presumed that the mixing of empty and filled orbital of the doped hetero atoms with the energetically coordinated valence and

conduction band orbital results in the broadening of the VB and CB. Besides, there are a few theoretical reports including our recent theoretical results that demonstrate the doping of these non-metals on TiO₂ lattice results in broadening at the top of the valence band, due to the contribution of 2p or 3p orbital of doped hetero-atom [4, 21-26]. Indeed, the position of hetero-atom in the lattice plays a major role in the band structure and position. In the case of TiO₂, there are two different sites (interstitial and substitutional) possible for doping. Conclusively, the doping of hetero-atom in the substitutional position in to the TiO₂ lattice alters the band more efficiently rather than the doping into the interstitial position. Also, the visible light photocatalytic activity depends on the concentration of the doped N- atoms [27]. There are a significant number of experimental reports on the preparation of N-doped TiO₂ [28-32]. In general, the preparation of N-doped TiO₂ has been successfully achieved either by reduction using gaseous NH₃, oxidation of TiN, decomposition of TiO₂ and urea mixture, sputtering of the TiO₂ target in N₂ atmosphere, or by hydrolysis of a titanium-dioxide precursor with NH₃ solution. In all these methods, the amount of nitrogen doped on the TiO₂ lattice by replacing the O atom in the lattice is limited due to the more stable Ti-O bond. In order to circumvent this problem, various other methods have also been developed by oxidative decomposition of direct Ti-N bond enriched Ti precursor. Sano *et al* [33] reported the preparation of N-TiO₂ by thermal decomposition of Ti⁴⁺-bipyridine complex and the photocatalytic removal of NO_x in visible light. Though, there is no clear evidence for the N doping in the TiO₂ lattice, extension of light absorption to the visible region and the visible light photocatalytic activity confirmed the doping of N in the TiO₂ lattice. In our earlier studies, we have reported the preparation of N-TiO₂ and N, S, co-doped TiO₂ by

oxidative decomposition of Ti- Salen based metal complex, and the visible light activity has also been proved by decomposition of methylene blue [34, 35]. It is found that calcination temperature has crucial role on the amount of N content in the TiO₂ lattice. So, the optimization of decomposition temperature is essential to achieve N-doped TiO₂ with maximum N content and the complete decomposition of precursor to attain maximum photocatalytic activity.

In the present study, an attempt has been made for the preparation of N-doped TiO₂ by oxidative decomposition of Ti-melamine complex. The photocatalytic activity of the N-doped TiO₂ samples have been investigated in the visible region for the decomposition of methylene blue as a model pollutant. The Ti-melamine complex has more number of Ti-N bonds with less number of carbons compared to other Ti-based metal complex. So, it is presumed that N-doped TiO₂ with higher amount of N content can be attained by oxidative decomposition.

Experimental

The Ti-melamine complex was prepared by mixing melamine in a hot water-ethanol mixture (1:3 volume ratio, ~50 °C) with titanium isopropoxide [Ti (ipro)₄] in ethanol solution. The ratio between the molar concentration of Ti (ipro)₄ and melamine in the mixture was maintained as 3:1 respectively. The resulting solution was stirred for 24 h and allowed to age for 5 days. The gel obtained after five days was dried in hot air oven, calcined at various temperatures in air for 4 h and finally washed with hot water. The

samples calcined at 400, 500, 600 and 700°C were designated as NT4, NT5, NT6 and NT7 respectively in the subsequent discussions.

UV-Visible absorption spectra were recorded using a CARY 5E UV-Vis-NIR spectrophotometer in the spectral range of 200-800 nm. The absorption spectra for the samples were recorded as a nujol paste. Powder X-ray diffraction patterns of the TiO₂ samples were recorded in a SHIMADZU XD-D1 diffractometer using Ni-filtered Cu K_α radiation ($\lambda = 1.5418 \text{ \AA}$). The chemical nature of N in TiO₂ was studied using X-ray photoelectron spectroscopy (XPS) in a VG Microtech Multilab ESCA 3000 spectrometer with a non-monochromatized Al K_α X-ray ($h\nu = 1486.6 \text{ eV}$). The catalyst pellet surface was scraped *in situ* to remove any surface contamination that could arise from atmospheric components like water, CO₂ etc. The energy resolution of the spectrometer was set at 1.1 eV at a pass energy of 50 eV. Binding energy (BE) was calibrated with respect to Au 4f_{7/2} core level at 83.9 eV. Specific surface area and pore volume of the samples were estimated from N₂ adsorption at 77 K using a SORPTOMETRIC (Model 1990) instrument. Prior to adsorption of N₂, the samples were degassed at 423 K for 12 h. Transmission Electron Micrographs (TEM) were recorded with a JEOL-JEM 100SX microscope, working at a 100 kV accelerating voltage.

Photocatalytic decomposition of methylene blue was performed on these materials using a quartz reactor with water circulation facility at the outer wall of the reactor and with a specific outlet for the sample collection. For a typical photocatalytic experiment, 0.1 g of catalyst was added to 50 ml of aqueous solution containing ~50 ppm of methylene blue

solution. The solution was irradiated using 400 W Hg lamp as light source and HOYA L-42 UV cut off filter to cut off the entire UV region (below 390 nm) and permit only the visible light. The experiments were carried out for a duration of 3 hrs. The catalyst was recovered by centrifuging and the light absorption of the clear solution was measured at 662 nm (λ_{\max} for MB). Prior to the experiment, the MB solution was stirred in the dark for 30 min and the adsorption of MB was measured. The resultant (un-adsorbed MB) concentration has been taken as initial concentration and the measured concentration at the different time intervals (during the reaction) were normalized to 50ppm. The photocatalytic activity was compared with those using commercial degussa (P25) photocatalyst and pure TiO₂ (anatase) prepared in the laboratory after normalizing for the MB adsorption.

Results and discussion

The thermal decomposition profile (TG) of Ti- melamine and pure melamine in air are shown in Fig. 1. The decomposition temperature of pure melamine was observed in the range of 320 to 350 °C, whereas Ti-melamine complex showed three regions 50-150, 300 to 450 and 550-700 °C, in total. In the temperature range studied (25 – 800⁰ C) only 40 % weight loss has been observed. It is believed that the weight loss in the first region is due to the adsorbed water and the second region is due to the decomposition of free non-complexed melamine. The weight loss in the third region could be ascribed to the decomposition of residuals, which are formed during the oxidation of melamine. The TG profile of air calcined samples NT4, NT5 and NT6 are shown in Fig 1. It shows negligible weight loss in the measured region, this indicates the complete decomposition

of the Ti-melamine complex and unbounded/adsorbed melamine on the prepared TiO₂ surface. Whereas, the samples decomposed at 300 °C and 200 °C show more than 50 - 60 % weight loss (not shown) at above 400 °C, which indicates the incomplete decomposition of TiO₂ precursor material at calcinations temperatures below 400 °C.

The UV-visible absorption spectra of N-doped TiO₂ and bulk TiO₂ samples are shown in Fig. 2. It can be seen from the figure that there is a significant shift in the onset absorption towards the higher wavelength region (~120 nm) for N-doped samples when compared to undoped TiO₂. Indeed, the absorption spectrum of NT4 and NT5 are comparable to one another, and the sample NT6 shows comparatively less shift in the onset absorption. Whereas, the sample NT7 show much lower shift in the onset absorption compared to other N- doped samples. This can be attributed to the reduction in the nitrogen content of the doped samples due to higher calcination temperature. It is well known from the literature that the calcination temperature plays a significant role in the amount of hetero atom doping [31, 35]. Unlike the N-doped TiO₂ prepared by salen complex [34], the decrease in the visible light response for the present catalyst with temperature is diminutive and significant amount of N-doping could be seen even at 700 °C calcination. Thermal decomposition of titanium complex with more number of Ti-N bonds will result with more amount of N-doping. Certainly, the increase in the calcination temperature leads to a lowering in the amount of hetero-atom doping. The effect of temperature generally varies with respect to the number of Ti-N bonding and the nature of preparation method adopted for the hetero-atom doping.

From the onset of the adsorption edge, the band gap of the N-doped TiO₂ particles was calculated using the method adopted by Tandon and Gupta [36]. The calculated band gap value is reduced by about 0.7eV for the NT4 and NT5 samples compared to bulk TiO₂. This observation clearly indicates that the doping of hetero-atom results in the formation of addition energy levels above the valence band of TiO₂. It is well known that, the valence and conduction bands of TiO₂ are mainly formed due to the major contribution by completely filled oxygen 2p orbital and the empty Ti 3d orbital, respectively. Our earlier studies and literature reported methods on hetero atom doped TiO₂ support the above observation that, due to energy equality, the 2p orbital of the doped N atom are significantly interacting with O 2p orbital and contributing to the valence band formation thereby the band width of the valence band increases significantly [4, 25].

Fig. 3 shows the X-ray diffraction pattern of bulk and N-doped TiO₂ samples. The presence of anatase phase has been observed for the bulk TiO₂ and NT4 and NT5 samples. When the calcination temperature is increased to 600 °C, formation of rutile phase, a high temperature phase, can also be seen (shown as “R”) in Fig. 3. The peak intensities corresponding to rutile phase are enhanced when the calcination temperature is increased further. It can be seen from Fig.3 that NT7 sample shows rutile phase predominantly with small amount of anatase crystalline feature. Irrespective of the calcination temperature, all the N-doped samples show X-ray line broadening compared to bulk TiO₂, representing the formation of nanoparticles. The extent of line broadening decreased with respect to increase in the calcination temperature, indicating the agglomeration of nanoparticle in the higher temperature. The calculated “d” values 3.51,

3.23, 2.47, 2.37, 1.89 and 2.17 for the N-doped samples are in good agreement with the anatase (JCPDS File No. 21-1272) and crystalline rutile (JCPDS File No. 21-1276) phase. No significant changes in the “d” values are observed, which indicates that the doping of N in the TiO_2 lattice does not alter the average unit cell dimension. It is worthwhile to point out here that the decomposition of Ti-N bond containing metal complex possibly results in the substitutional doping of N in the TiO_2 lattice rather than interstitial doping.

The surface morphology of the N-doped TiO_2 nanoparticle has been studied by scanning electron microscopy. The SEM images of the NT4 sample with two different magnifications are presented in Fig. 4. The growth of mixture of spherical and flakes like particles of N-doped TiO_2 can be clearly seen from the images. The different morphology of the observed N- TiO_2 particle could be attributed to the decomposition of Ti-melamine complex and other partial metal complex. The TEM image of the N-doped TiO_2 sample (NT4) is shown in Fig. 5. Particles in nanosize range could be seen clearly for the N-doped TiO_2 sample. In addition, the presence of spherical type particles also can be seen clearly from the TEM. There is a good concordance between the SEM and TEM images for the N-doped sample that the particle morphology could be seen as spherical in both the image. However, the flakes like particle have not been observed in the TEM. The particle size of the spherical particle sample (NT4) has been calculated to be approximately 25 nm from the micrograph.

The chemical state of the doped nitrogen in the TiO_2 has been studied by X-ray photoelectron spectroscopy and shown in Fig 6. Fig 6a shows the service spectrum of N-

doped TiO₂ (NT4), the presence of N in the TiO₂ could be seen from the BE peak around 400 eV. A rescaled plot is shown in Fig. 6b (black line). A broad peak centered at 400 eV could be seen for the NT4 sample. On deconvolution, it can be seen that the broad peak consists of four different peaks at 396.2, 398.4, 400 and 401.5 eV are discernible. The observed peak at 396.2 eV is attributed to the presence of Ti-N bond in the TiO₂ lattice [4, 30]. The observed peak at 398.4 eV is due to the presence of nitrogen in the N-Ti-O environment [37, 38, 31]. Based on the reports of Saha *et al* [39] and Gyorgy *et al* [40], the BE of N in an oxidized nitrogen such as Ti-N-O linkages should appear above 400 eV. The observed peak at 401.3 eV accounts for the presence of oxidized state of N as NO or NO₂ in the N-doped TiO₂ sample. This can be attributed to the decomposition of unbound melamine molecule chemically adsorbed on the Ti-melamine complex or the decomposition of oxidized Ti-melamine complex residue. It is well known from the literature that, in some cases of N-doped TiO₂, the peak at 396.2 eV appears only after Ar⁺ etching and this observation has been credited to the oxidation of doped N atoms present in the surface and near the surface. The above explanation accounts for the peak observed at 401.3 eV in our present study. Also, the presence of N as adsorbed N₂ like species on the surface of the sample could be seen from the peak observed at a BE lower than of 400 eV. The present results are in accordance with the values reported in the literature for N doped TiO₂ sample [38, 39, 41].

There is a noticeable shift in the Ti⁴⁺ binding energy towards lower binding energy region due the slightly reduced oxidation state. However, there is no clear evidence for the formation two different types of Ti species in the doped samples. This indicates that the

overall charge of the Ti^{4+} ion is slightly reduced due to doping of N atom in the TiO_2 lattice. A similar observation in N doped TiO_2 by N^+ ion bombardment has been reported by Nambu *et al* [42]. Further, our previous result confirms the reduction in the oxidation state of Ti^{4+} due to the doping of N atoms [31].

The visible light decomposition profile of methylene blue over N-doped samples is shown in Fig. 7. It can be seen that, there is a significant change in the decomposition of methylene blue as the temperature of calcinations is increased to 600 °C. The rate of decomposition is high in the case of sample calcined at 500 °C, compared to other two samples. It is speculated that the lower rate of decomposition of methylene blue, for 600 °C calcined sample, is due to either one or combination of the following factors: (i) decreased visible light absorption capability of the catalyst due to less amount of N in the NT6 compared to NT4 and NT5. (ii) The formation of less photoactive rutile phase due to high calcination temperature. The UV-visible absorption spectrum of the sample NT6 supports for our earlier speculation. Nevertheless, comparing 400 and 500 °C calcined samples, the latter is more active than the former due to a higher crystalline nature (anatase). In conclusion, ~ 40 % of methylene blue decomposition is achieved by the N-doped TiO_2 sample, in the visible region alone, within 3h. Whereas, in UV + Visible region, complete decomposition of methylene blue has been achieved within 1 h for the 400 °C calcined N-doped TiO_2 samples (Fig. 8). The photocatalytic decomposition profile of methylene blue in the visible and UV+Visible region on NT4 has been compared with the N-doped TiO_2 (TS) prepared from decomposition of Ti-salen complex, which has been reported in our earlier study [34]. The photocatalytic

experimental conditions of the TS sample have been normalized with the present experimental conditions. Though the calcination temperature is the same for both the N-doped TiO₂ samples, the NT4 shows more photocatalytic activity than the TS. The lesser photocatalytic activity of TS compared to NT4 could be attributed to the low amount of N-doping in TS sample. As the number of Ti-N bonding in the Ti-salem complex is lower than Ti-melamine complex. This comparison clearly indicates that the nature of the metal complex, number of Ti-N bond and decomposition temperature has vital role on the N-doping and the resulting photocatalytic activity.

Conclusions

Nitrogen doped spherical TiO₂ has been prepared by thermal decomposition of Ti-Melamine complex. The prepared N-doped TiO₂ sample shows the light absorption onset in the visible region. The extent of light absorption in the visible region depends on the content of N in the N-doped TiO₂ samples, which varies with calcination temperature. The TEM and SEM images show a mixture of spherical-shaped and flake like particles with an average size of 25-50 nm. The XRD patterns of the N-doped samples confirm the presence of crystalline anatase TiO₂ nanoparticle below 500 °C. At temperatures above 500 °C, the less photoactive rutile crystalline phase begins to appear along with the anatase phase. The XPS studies reveal that the N exists as an anion, like in the doped samples and possibly the doped N occupies the oxygen position in the TiO₂ lattice. The observed XPS result also supports the possibility of survival of N-Ti-O environment in the N-doped TiO₂ samples. The visible light photocatalytic activity have been studied by methylene blue decomposition and estimated to be ~ 40 % decomposition for the N-

doped samples. The N-doped TiO₂ prepared from the Ti-melamine complex precursor shows higher activity than the N-doped TiO₂ prepared by Ti-salen complex precursor.

Acknowledgement:

We thank the Department of Science and Technology (DST), New Delhi, for funding the research and University Grant Commission (UGC) New Delhi, for fellowship to one of the authors, M. Sathish.

References

1. A. Fujishima, K. Honda, *Nature* 238 (1972) 37.
2. M. Herrmann, J. Disdier, P. Pichat, *Chem. Phys. Lett.* 108 (1984) 618.
3. K.E. Karakitsou, X. E. Verykios, *J. Phys. Chem.* 97 (1993) 1184.
4. R. Asahi, T. Morikawa, T. Ohwaki, K. Aoki, Y. Taga, *Science* 293 (2001) 269.
5. J.L. Gole, J.D. Stout, C. Burda, Y. Lou, X. Chen, *J. Phys. Chem. B* 108 (2004) 1230.
6. S. Sakthivel, H. Kisch, *Angew. Chem. Int. Ed.* 42 (2003) 4908.
7. T. Umebayashi, T. Yamaki, S. Tanaka, K. Asai, *Chem. Lett.* 32 (2003) 330.
8. T. Ohno, T. Mitsui, M. Matsumura, *Chem. Lett.* 32 (2003) 364.
9. H. Irie, Y. Watanabe, K. Hashimoto, *Chem. Lett.* 32 (2003) 772.
10. M. Mrowetz, W. Balcerski, A.J. Colussi, M.R. Hoffmann, *J. Phys. Chem. B.* 108 (2004) 17269.
11. N. Serpone, *J. Phys. Chem. B.* 110 (2006) 24287.
12. S. Yin, K. Ihara, Y. Aita, M. Komatsu, T. Sato, *J. Photochem. Photobiol, A.* 179 (2006) 105.
13. J. Wang, W. Zhu, Y. Zhang, S. Liu, *J. Phys. Chem. C* 111 (2007) 1010.
14. S. Livraghi, M.C. Paganini, E. Giamello, A. Selloni, C.D. Valentin, G. Pacchioni, *J. Am Chem. Soc.* 128 (2006) 15666.

15. T. Ihara, M. Miyoshi, Y. Iriyama, O. Matsumoto, S. Sugihara, *Appl. Catal. B.* 42 (2003) 403.
16. R. Silveyra, L.D.L.T. Sa'enz, W.A.Flores, V.C. Marti'nez, A.A. Elgue'zabal, *Catal.Today* 107–108 (2005) 602.
17. O. Diwald, T.L. Thompson, T. Zubkov, Ed.G. Goralski, S.D. Walck, John T. Yates, Jr. *J. Phys. Chem. B* 108 (2004) 6004.
18. Y. Suda, H. Kawasaki, T. Ueda, T. Ohshim, *Thin Solid Films* 453–454 (2004) 162.
19. R. Bacsa, J. Kiwi, T. Ohno, P. Albers, V. Nadtochenko, *J. Phys. Chem. B.* 109 (2005) 5994.
20. Y.C. Hong, C.U. Bang, D.H. Shin, H.S. Uhm, *Chem. Phys. Lett.* 413 (2005) 454.
21. C.D. Valentin, G. Pacchioni, A. Selloni, *Chem. Mater.* 17 (2005) 6656.
22. T. Umebayashi, T. Yamaki, S. Yamamoto, A. Miyashita, S. Tanaka, T. Sumita, K. Asai, *J. Appl. Phys.* 93 (2003) 5156.
23. T. Umebayashi, T. Yamaki, H. Itoh, K. Asai, *Appl. Phys. Lett.* 81 (2002) 454.
24. T. Ohno, M. Akiyoshi, T. Umebayashi, K. Asai, T. Mitsui, M. Matsumura, *Appl. Catal. A.* 265 (2004) 115.
25. M. Sathish, PhD Thesis, IIT-Madras (2006)
26. F. Tian, C. Liu, *J. Phys. Chem. B.* 110 (2006) 17866.
27. H. Irie, Y. Watanabe, K. Hashimoto, *J. Phys. Chem. B.* 107 (2003) 5483.
28. S. Yang, L. Gao, *J. Am. Ceram. Soc.* 87 (2004) 1803.
29. S. Sakthivel, M. Janczarek, H. Kisch, *J. Phys. Chem. B.* 108 (2004) 19384.
30. K. Kobayakawa, Y. Murakami, Y. Sato, *J. Photochem. Photobiol. A.* 170 (2004) 177.
31. M. Sathish, B. Viswanathan, R.P. Viswanath, C.S. Gopinath, *Chem. Mater.* 17 (2005) 6349.
32. W. Ren, Z. Ai, F. Jia, L. Zhang, X. Fan, Z. Zou, *Appl. Catal. B.* 69 (2007) 138.
33. T. Sano, N. Negishi, K. Koike, K. Takeuchi, S. Matsuzawa, *J. Mater. Chem.* 14, (2004) 380.

34. M. Sathish, B. Viswanathan, R.P. Viswanath. *Int. J. Nanoscience (under publication)*
35. M. Sathish, R.P. Viswanath, C.S. Gopinath (to be communicated)
36. S.P. Tandon, J.P. Gupta, *Physica Status Solidi*. 38 (1970) 363.
37. X. Chen, C. Burda, *J. Phys. Chem. B*. 108 (2004) 5446.
38. H. Li, J. Li, Y. Huo *J. Phys. Chem. B*. 110 (2006) 1559.
39. N.C. Saha, H.G. Tompkins, *J. Appl. Phys.* 72 (1992) 3072.
40. E. Gyorgy, A. Perez del Pino, P. Serra, J.L. Morenza, *Surf. Coat. Technol.* 173 (2003) 265.
41. Y. Nosaka, M. Matsushita, J. Nishino, A.Y. Nosaka, *Science and Technology of Advanced Materials* 6 (2005) 143.
42. A. Nambu, J. Graciani, J.A. Rodriguez, Q. Wu, E. Fujita, J.Fdez Sanz, *J. Chem. Phys.*, 125 (2006) 094706.

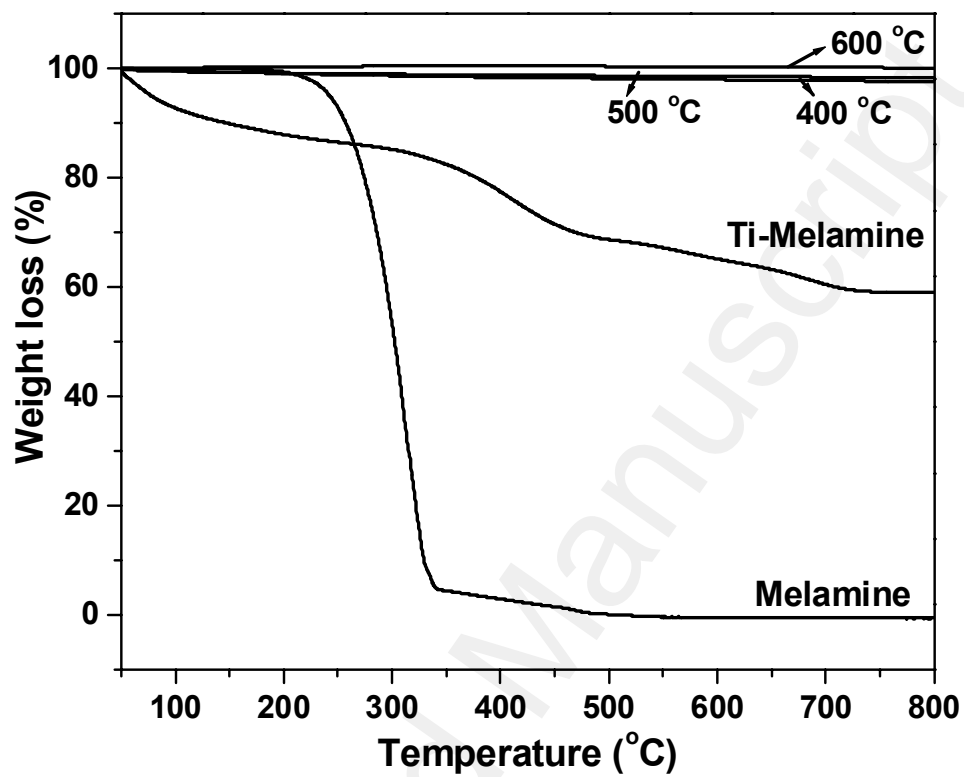


Figure 1. TGA profile of melamine, Ti-Melamine and N-TiO₂ calcined at 400, 500 and 600 °C

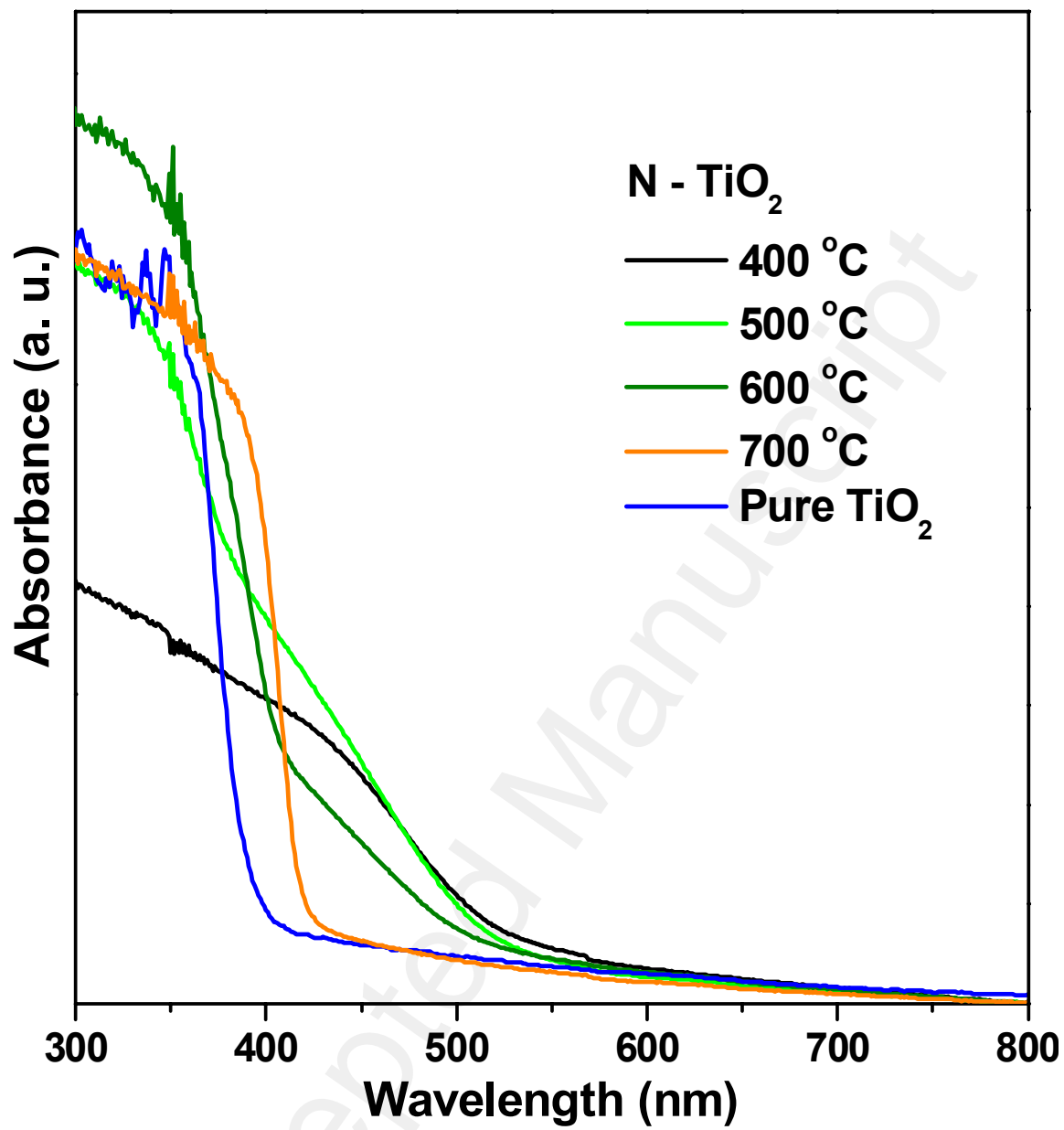


Figure 2. UV-Visible absorption spectrum of N-doped TiO₂ at different calcination temperatures and pure TiO₂

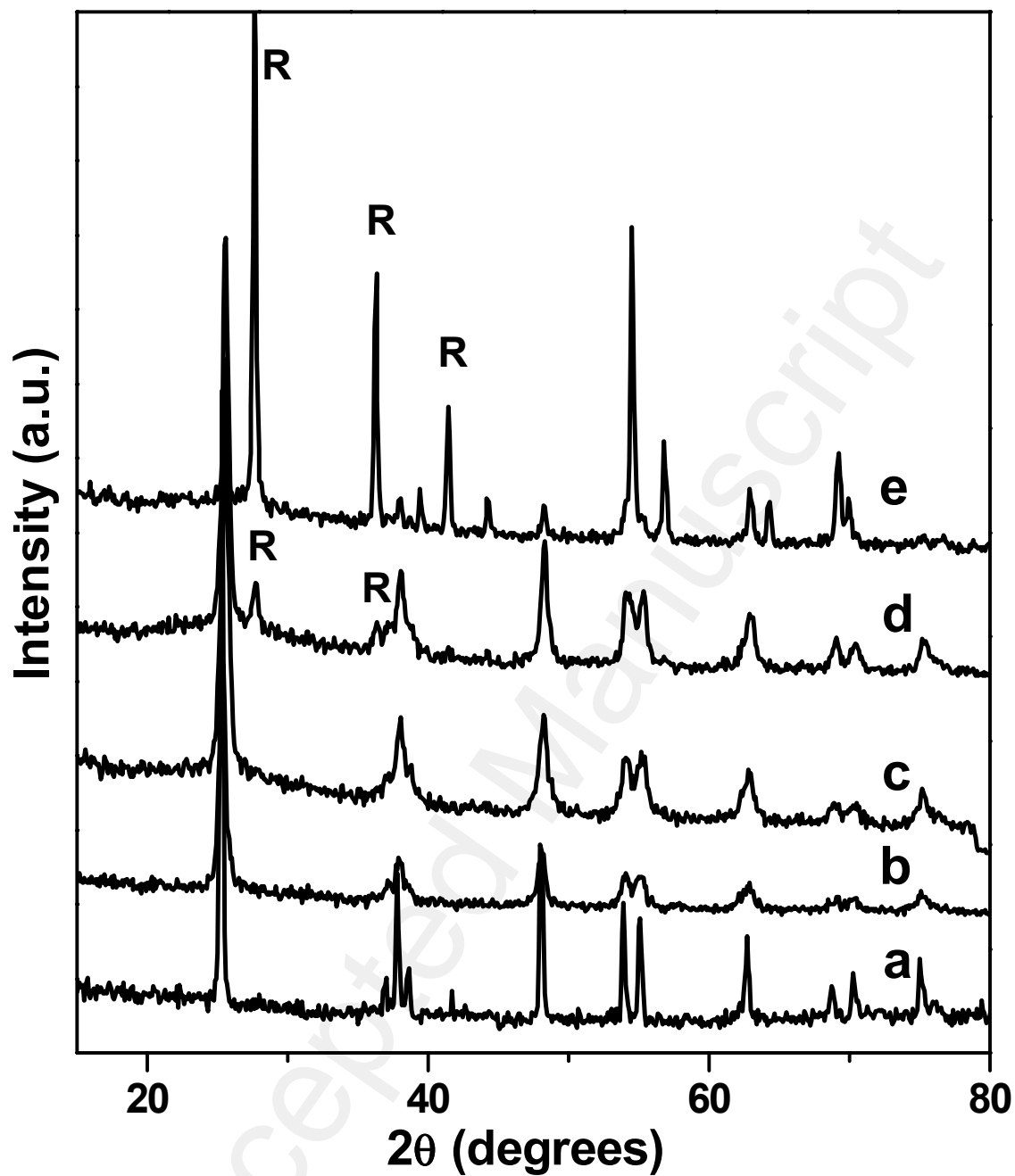
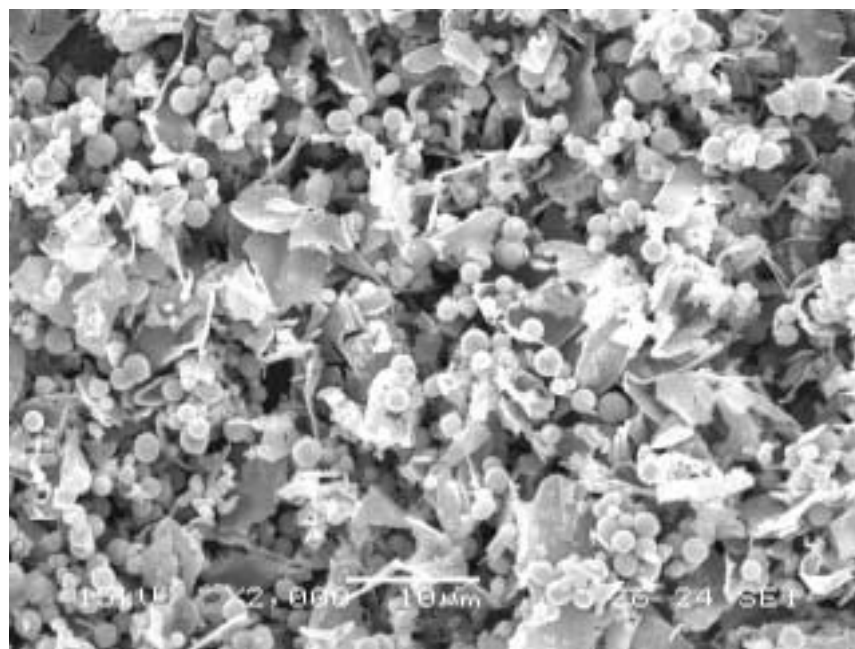
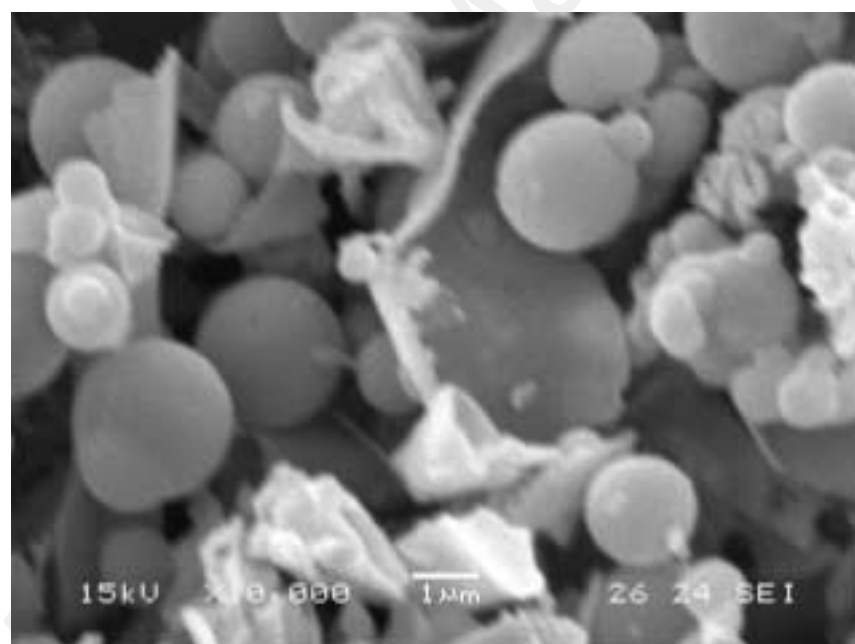


Figure 3. X-ray diffraction patterns of (a) pure anatase TiO_2 and N-doped TiO_2 calcined at different temperatures (b) NT4 (c) NT5 (d) NT6 and (e) NT7



(a)



(b)

Figure 4. SEM image of N-doped TiO_2 (NT4)

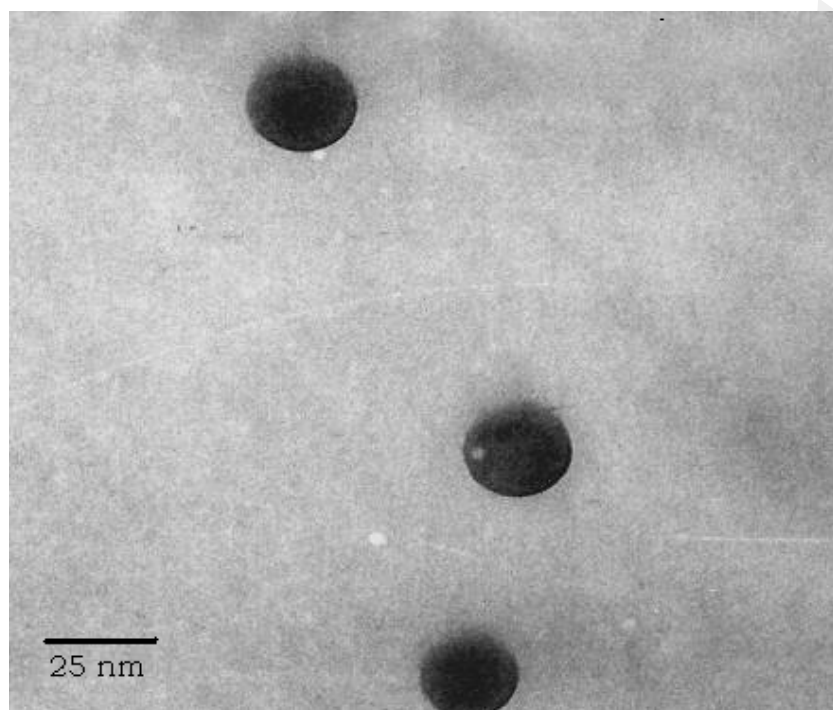
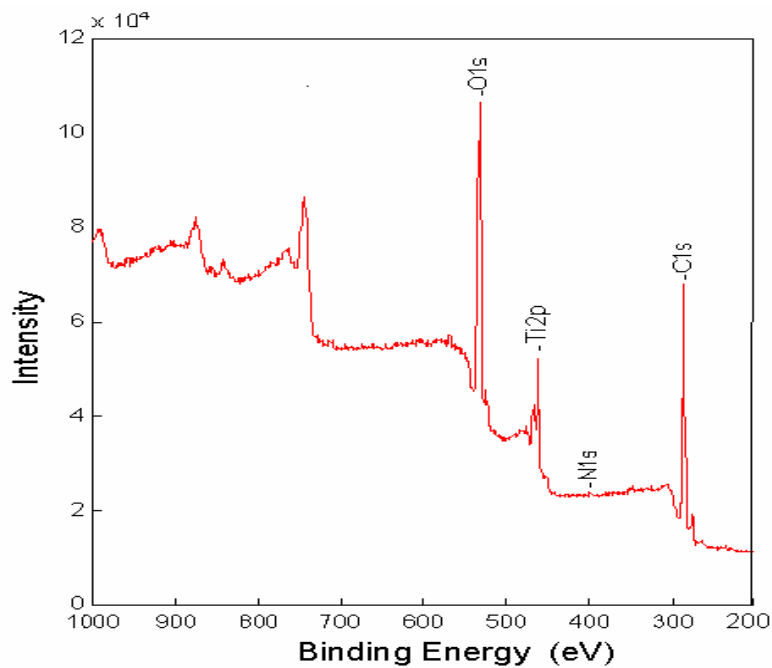
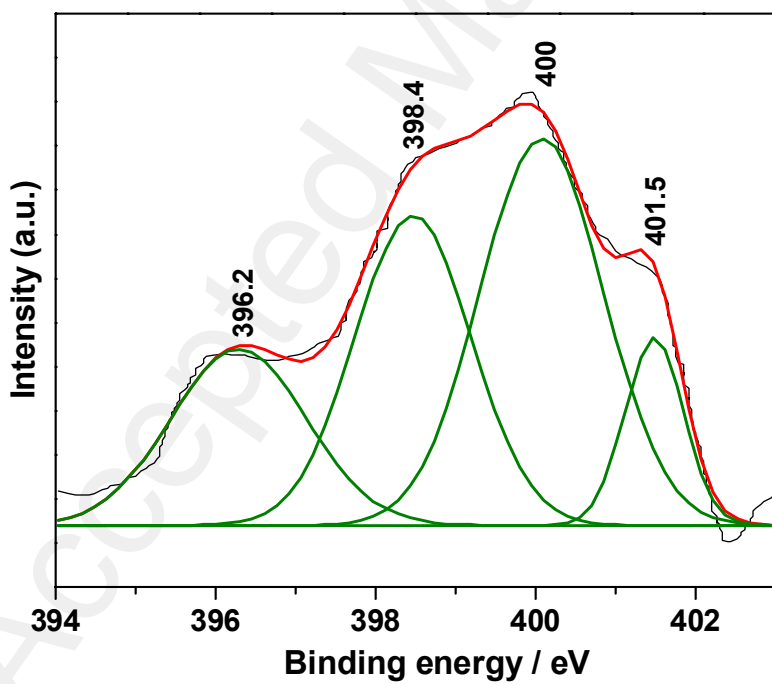


Figure 5. TEM image of N-doped TiO₂ (NT4)



(a)



(b)

Figure 6. X-ray photoelectron spectrum of (a) N-TiO₂ and (b) N 1s levels for N-TiO₂ sample (NT4)

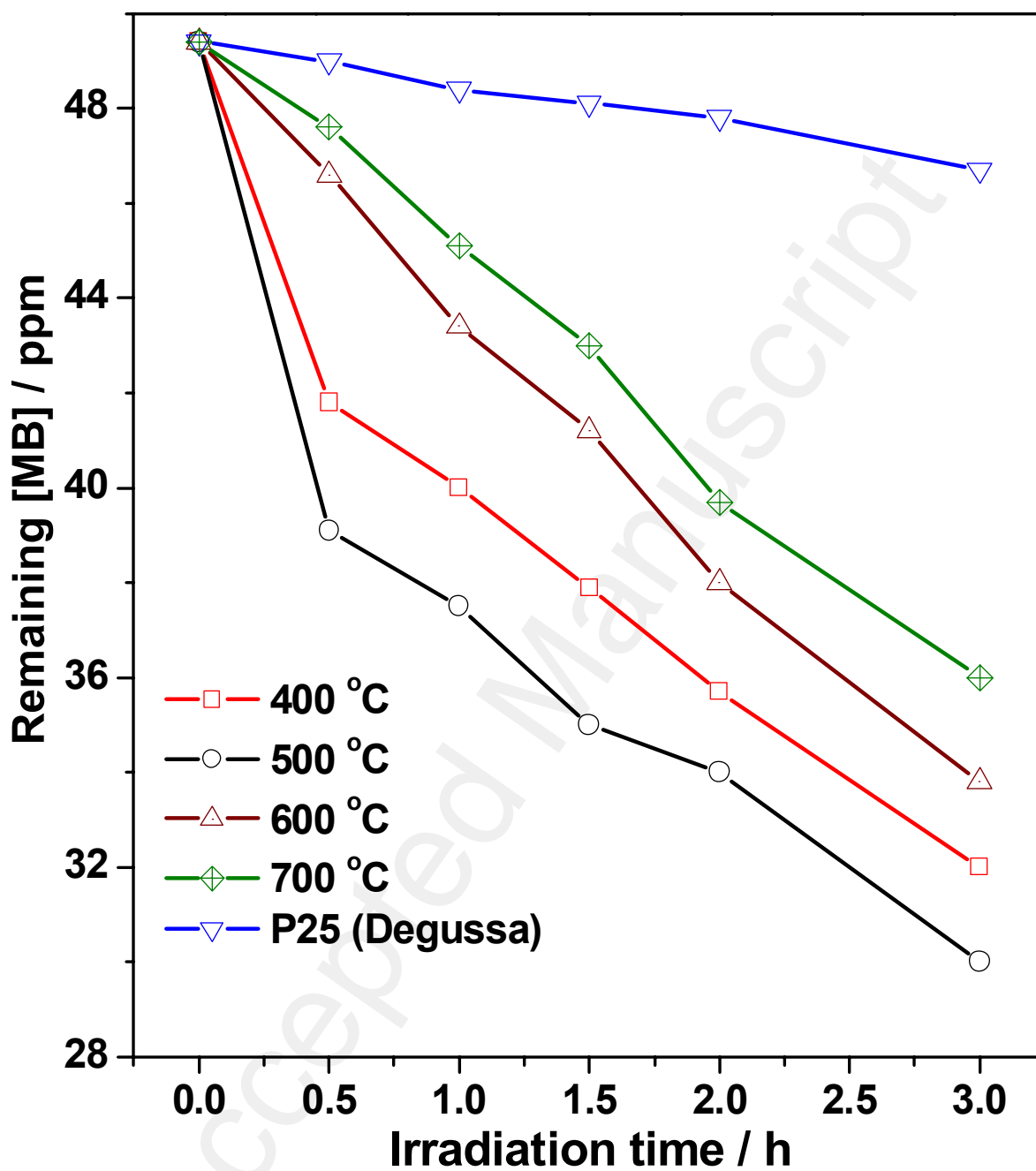


Figure 7. Photocatalytic decomposition profile of methylene blue over N-doped TiO₂ calcined at different temperatures and Degussa (P25) in the visible light.

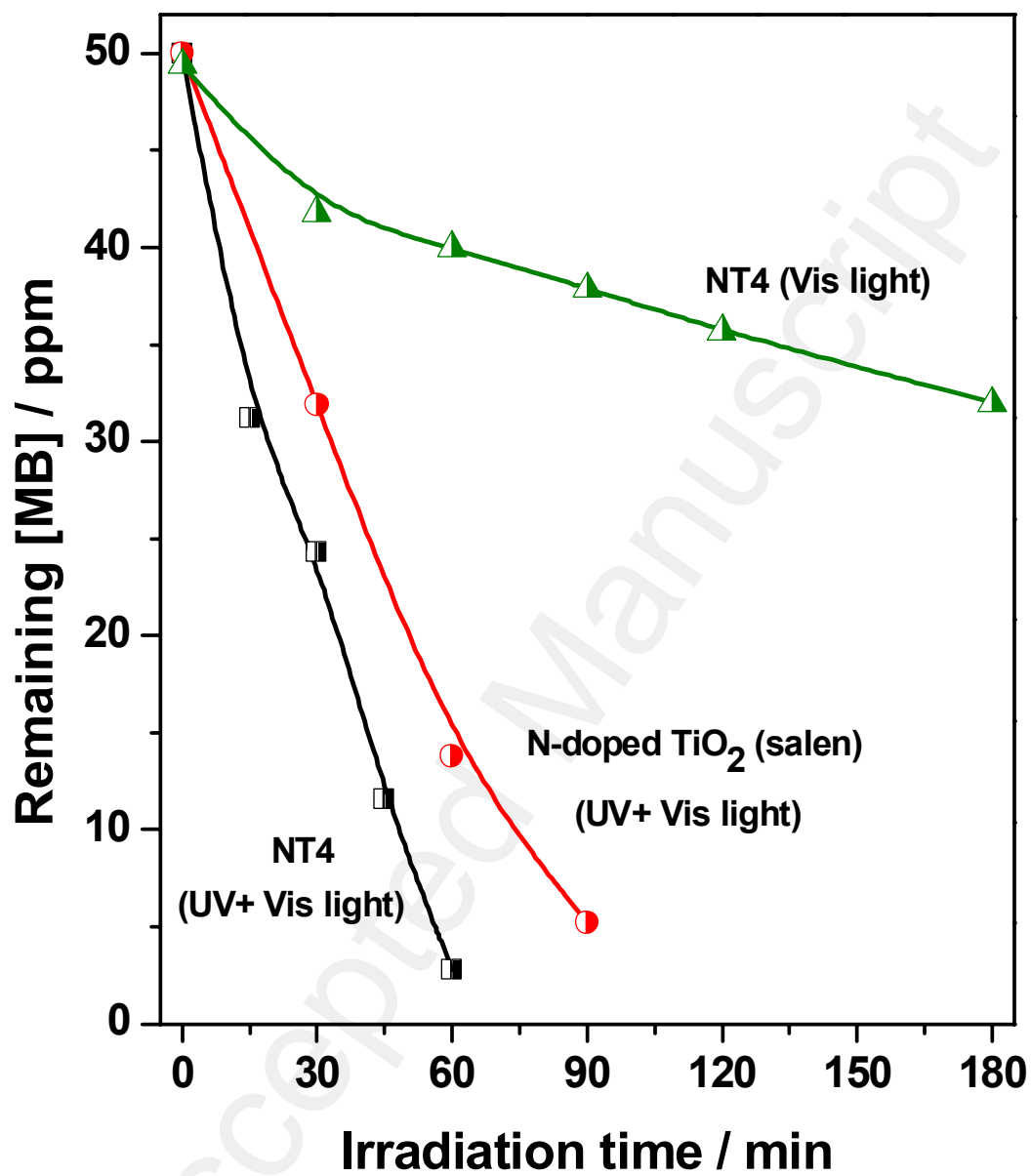


Figure 8. Photocatalytic decomposition profile of methylene blue over NT4 (UV+ Vis light), NT4 (Vis light) and N-doped TiO₂ (salen) (UV+ Vis light)